Am J Transl Res 2016;8(6):2498-2511
www.ajtr.org /ISSN:1943-8141/AJTR0028974

Original Article

Extracellular matrix metalloproteinase inducer (CD147/BSG/EMMPRIN)-induced radioresistance in cervical cancer by regulating the percentage of the cells in the G2/m phase of the cell cycle and the repair of DNA Double-strand Breaks (DSBs)

Xingzhu Ju, Shanhui Liang, Jun Zhu, Guihao Ke, Hao Wen, Xiaohua Wu

Department of Gynecologic Oncology, Fudan University Shanghai Cancer Hospital, Shanghai, China

Received March 23, 2016; Accepted May 10, 2016; Epub June 15, 2016; Published June 30, 2016

Abstract: Our preliminary study found that CD147 is related to radioresistance and maybe an adverse prognostic factor in cervical cancer. To date, the mechanisms underlying CD147-induced radioresistance in cervical cancer remain unclear. In the present study, we investigated the mechanisms by which CD147 affects radiosensitivity in cervical cancer both in vitro and in vivo. In this study, the clonogenic assay showed that radiosensitivity was significantly higher in the experimental group (the CD147-negative cell lines) than in the control group (the CD147-positive cell lines). After radiotherapy, the residual tumour volume was significantly lower in the experimental group. FCM analysis showed the cells percentage in the G2/M phase of the cell cycle were significantly higher in the CD147-negative group than in the control group. However, there was no significant difference in terms of apoptosis. The expression of gamma-H2A histone family, member X (γH2AX) was dramatically elevated in the CD147-negative cell lines after irradiation, but the expression of ataxia-telangiectasia mutated (ATM) was not different between the two groups. WB analysis did not show any other proteins relating to the expression of CD147. In conclusion, it is likely that CD147 regulates radioresistance by regulating the percentage of the cells in the G2/M phase of the cell cycle and the repair of DNA double-strand breaks (DSBs). Inhibition of CD147 expression enhances the radiosensitivity of cervical cancer cell lines and promotes post-radiotherapy xenograft tumour regression in nude mice. Therefore, CD147 may be used in individualized therapy against cervical cancer and is worth further exploration.

Keywords: Cervical cancer, radiosensitivity, extracellular matrix metalloproteinase inducer, DNA double-strand breaks

Introduction

Cervical cancer is the most common malignancy of the female reproductive system. Approximately 500,000 new cases of cervical cancer are reported every year worldwide [1]. Eighty percent of cervical cancer cases occur in developing countries, including China. In China, approximately 130,000 new cases of cervical cancer are diagnosed every year [2]. More than 50% of cervical cancer patients have cancers that are already at an advanced stage at the time of diagnosis, and chemoradiotherapy has become the only treatment option, and the five-year survival rate is less than 50% for these advanced stage patients. More than 70% of relapses occur within the first 2 years after treatment. The most common site of recurrence is within the pelvic radiation field. The insensitivity of tumour cells to radiotherapy is the main reason for treatment failure [3, 4]. Therefore, investigating the mechanisms underlying tumour cell radioresistance, seeking predictors of radiosensitivity, identifying patients with radioresistant tumours, and developing targeted therapies and radiosensitization strategies aimed at radioresistance factors are the foci of clinical and basic cervical cancer studies.

Extracellular matrix metalloproteinase inducer (EMMPRIN/CD147) is a member of the immunoglobulin superfamily. The expression of

CD147 is increased in tumour cells, and this increase is correlated with invasion, metastasis, drug-resistance and other malignant behaviours in a variety of malignant tumours [5]. Targeted inhibition of CD147 expression in tumour cells inhibits tumour cell growth, reduces the invasive and metastatic capability of tumour cells, and increases the sensitivity of tumour cells to chemotherapy. Therefore, CD147 is a valuable therapeutic target [6, 7]. Our previous study found that CD147 is negatively correlated with the regression of cervical cancer after radiotherapy and may induce radioresistance in cervical cancer cells [8]. However, the underlying mechanisms remain unknown. The radiosensitivity of malignant tumour cells is related to DNA DSB repair [9], cell cycle distribution (G2/M phase arrest) [10, 11], apoptosis [12] and metabolism under hypoxic conditions [13]. Therefore, in the present study, we attempted to explore the mechanisms underlying CD147-induced radioresistance in cervical cancer cells from these pathways and to further verify the relationship between CD147 and the radiosensitivity of cervical cancer through in vivo and in vitro experiments.

Materials and methods

Cells and cell culture

The cervical cancer cell lines ME-180 and SiHa were purchased from the American Type Culture Collection (ATCC) and the Shanghai Institute of Biochemistry and Cell Biology (SIBCB) of the Chinese Academy of Sciences (CAS), respectively. The cells were cultured in accordance with the suppliers' instructions.

Antibody sources

Rabbit anti-human CD147 antibody was purchased from BioLegend. Rabbit anti-human mammalian target of rapamycin (mTOR), cyclin D1, survivin, ataxia-telangiectasia mutated (ATM) and checkpoint kinase 2 (Chk2) antibodies were purchased from Epitomics. Rabbit anti-human cyclin-dependent kinase 2 (Cdk-2), hypoxia-inducible factor 1-alpha (HIF-1α), gamma-H2A histone family, member X (γH2AX), XRCC4-like factor (XLF) and beta-actin antibodies were purchased from Cell Signaling Technology (CST) Inc. All secondary antibodies, including goat anti-rabbit IgG and goat anti-mouse IgG, were purchased from CST Inc.

Examination of apoptosis by flow cytometry

(Annexin V-propidium iodide (PI) staining): Cell were seeded into 6-well plates at a density of 5×10^5 cells/well and cultured overnight. The cells were then trypsinized and centrifuged. After removal of the supernatant, the cells were resuspended in an appropriate buffer and labelled with fluorescein isothiocyanate (FITC)-conjugated Annexin V. Three test tubes were set up as controls.

Analysis of the cell cycle by flow cytometry

The cells were seeded into 6-well plates at a density of 5×10^5 cells/plate. After overnight cultivation, the cells were trypsinized and centrifuged. The supernatant was discarded, and the cells were resuspended in phosphate-buffered saline (PBS). Subsequently, the cells were fixed, centrifuged and stained with PI (a fluorescent DNA-intercalating dye). Cell cycle analysis was then conducted using flow cytometry.

Lentiviral packaging and construction of stably transduced cell lines

The lentiviruses used in the present study were packaged by Shanghai GenePharma Co., Ltd. Stable cell lines were constructed using the manufacturer's instructions. ME-180 and SiHa cells were cultured to 80-90% confluence in 10-cm dishes. After being treated with normal and standard solutions, the cells were pipetted to create a suspension of single cells. Then the cells were seeded evenly into 6-well plates at a density of 10×10^5 cells/well and cultured for 24 h at 37°C under an atmosphere of 5% CO_2. The culture medium in the 6-well plates was aspirated and replaced with the diluted viral solution (1 ml per well). A blank control group was set up at the same time. After incubation and being replaced coulture solution, once the cells reached 80-90% confluence in 6-cm dishes, puromycin was added to the cells at a concentration that was determined using the lethal dose test. A blank control group was set up at the same time. Until all cells in the blank control group were killed, cells that survived puromycin selection were considered stably transduced. After establishment of the stable cell lines, the cells were amplified, collected, and examined by polymerase chain reaction (PCR) and western blot (WB) analyses.

Real-time quantitative PCR (RT-PCR)

Total RNA were extracted using the manufacturer's instructions. Agarose gel electrophoresis was performed to examine the integrity of the RNAs. The RNA primers were provided by Shanghai GenePharma Co., Ltd. The reverse transcription (RT) reactions were set up as follows: 10 μl of RT buffer, 1.2 μl of RT primer, 0.2 μl of total RNA, and sufficient DEPC-treated water to bring the volume to 20 μl under reaction conditions of 42°C for 30 min and 85°C for 10 min. The fluorescence-based quantitative real-time PCR systems were set up as follows: 10 μl of Quantitative PCR Master Mix, 0.08 μl of upstream primer (20 μM), 0.08 μl of downstream primer (20 μM), 2 μl of complementary DNA (cDNA) template, 0.4 μl of Taq DNA polymerase (2.5 U/μl), and sufficient ddH_2O to bring the volume to 20 μl under reaction conditions of denaturation at 95°C for 3 min and 40 cycles of 95°C for 12 sec and 62°C for 40 sec.

Western Blot

The concentration of total cellular protein was determined using the Bicinchoninic acid (BCA) assay. The proteins were subjected to sodium dodecyl sulphate polyacrylamide gel electrophoresis (SDS-PAGE), transferred to polyvinylidene fluoride (PVDF) membranes, hybridized with antibodies and incubated overnight. Subsequently, electrochemiluminescence (ECL) reagent was dropped evenly onto each PVDF membrane (which was placed on a tray) until the membrane was fully immersed in the chromogenic reagent. After incubation for 1-2 min, the PVDF membranes were placed in an ImageQuant LAS 4000 gel imaging system and imaged using appropriate software. The images were analysed and processed using Gel-Pro Analyzer software.

Clonogenic assay

Cells that were seeded at a density of 5×10^5 cells/well in 6-well plates were trypsinized to form single-cell suspensions and counted. SiHa and ME-180 cells were seeded at 200, 500, 1,500, 4,000 and 6,000 cells per well and overlaid with 3 ml of complete medium. The cells were then statically cultured under 37°C, 5% CO2 and saturated humidity. The cells were subjected to radiotherapy (X-ray-beam energy, 6 MV) after adhering to the culture surface. The cells were irradiated at various doses (0, 2, 4, 6 and 8 Gy), and each dose was repeated 3 times. At 10-13 d after radiotherapy, clones visible to the naked eye appeared in the plates. The clones were washed , fixed and stained. The rates of clone formation were calculated, and survival curves were established. Clone formation rate (plating efficiency, PE) = number of clones/number of cells seeded × 100%. Surviving fraction (SF) = number of clones in an experimental group/(number of cells seeded × PE) × 100%. Experimental data for PE and SF were fitted using the multi-target single-hit model and the linear quadratic model, respectively. Survival curves were plotted.

Xenograft tumour formation in nude mice and radiosensitivity assay

Logarithmically growing SiHa and SiHa-1575 cells were harvested and dispersed into single-cell suspensions. Cell concentration was adjusted to 1×10^8 cells/ml. Twenty-four nude mice were randomly divided into two groups: group A and group B. Nude mice in group A were injected with 0.1 ml of SiHa cells in the right thigh, whereas nude mice in group B were injected with 0.1 ml of SiHa-1575 cells in the right thigh. On the 10th day after inoculation of the tumour cells (when the subcutaneous tumours had diameters of approximately 5 mm), the 12 mice in group A were randomly divided into 2 groups. One group received radiotherapy (16 Gy of 6-MV X-rays); the other group did not. Mice in group B were subjected to the same treatments. Tumour volume was measured every 3-5 d, and the data were recorded. On the 37th day after inoculation of the tumour cells, all mice were killed. Tumour volume growth curves were created. Tumour volume was calculated using the following formula: Tumour volume = (short diameter2 × long diameter)/2.

Statistical analysis

Statistical analysis was conducted using SPSS 19 statistical software. Intergroup differences were analysed using Student's t test. *P* values of less than 0.05 were considered statistically significant.

Results

Evaluation of CD147 expression of stable cell lines by RT-PCR and WB

RT-PCR and WB analyses of the stable cell lines were conducted. The parental ME-180 and SiHa cells expressed CD147. The cell lines that

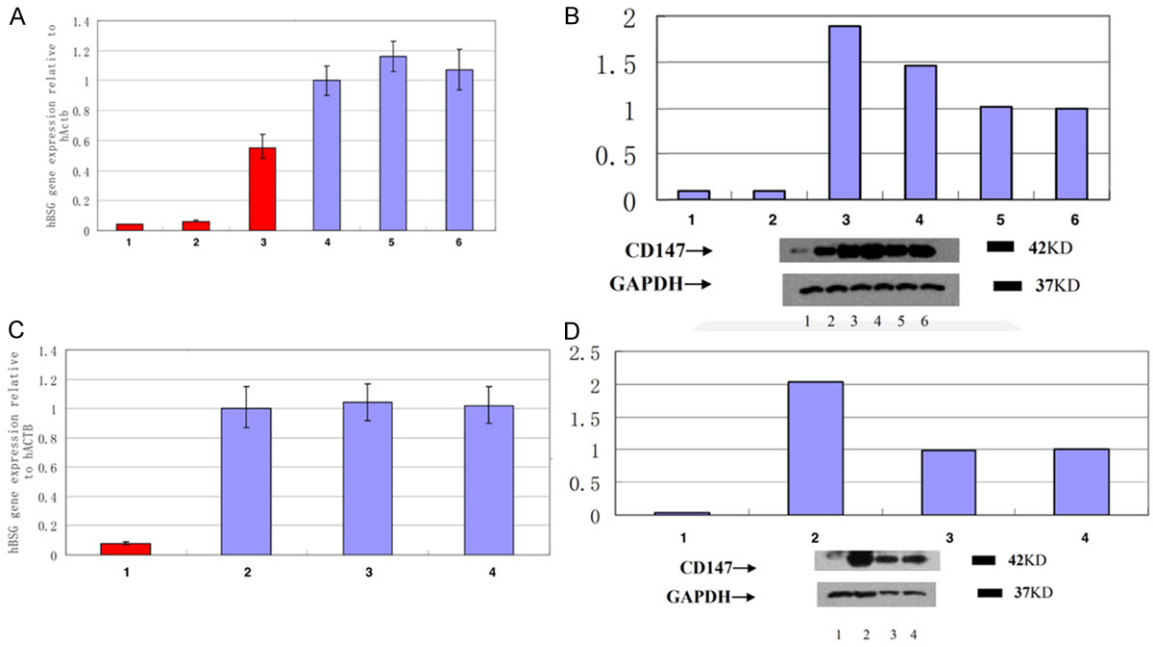

Figure 1. Evaluation of CD147 expression of stable cell lines by RT-PCR and WB. A. CD147 expression in various cell lines as determined by RT-PCR: 1 and 2, the shRNA-CD147-transduced CD147-negative cell lines ME-180-1575 and ME-180-1576; 3, the cDNA-CD147-transduced CD147-positive cell line ME-180-2459; 4, the control LV3-NC; 5, the blank control LV5-NC; and 6, untransduced parental ME-180 cells.The results shown are representative of 3 independent experiments. B. CD147 expression in various cell lines as evaluated by WB analysis: 1 and 2, the shRNA-CD147-transduced CD147-negative cell lines ME-180-1575 and ME-180-1576; 3, the cDNA-CD147-transduced CD147-positive cell line ME-180-2459; 4, the control LV3-NC; 5, the blank control LV5-NC; and 6, untransduced parental ME-180 cells. The cell lines that were stably transduced with lentivirus-carrying cDNA-CD147 (-2459 cell lines) expressed CD147 at levels similar to those of the parental cells. In contrast, short hairpin RNA (shRNA)-CD147 inhibited CD147 expression by more than 90% in both cell lines -1575 and -1576, so we selected -1575 as experimental group.The results shown are representative of 3 independent experiments. C. CD147 expression in various cell lines as determined by RT-PCR: 1, the shRNA-CD147-transduced CD147-negative cell line SiHa-1575; 2, the cDNA-CD147-transduced CD147-positive cell line SiHa-2459; 3, the blank control LV5-NC; and 4, untransduced parental SiHa cells.The results shown are representative of 3 independent experiments. D. CD147 expression in various cell lines as evaluated by WB analysis: 1, the shRNA-CD147-transduced CD147-negative cell line SiHa-1575; 2, the cDNA-CD147-transduced CD147-positive cell line SiHa-2459; 3, the blank control LV5-NC; and 4, untransduced parental SiHa cells.

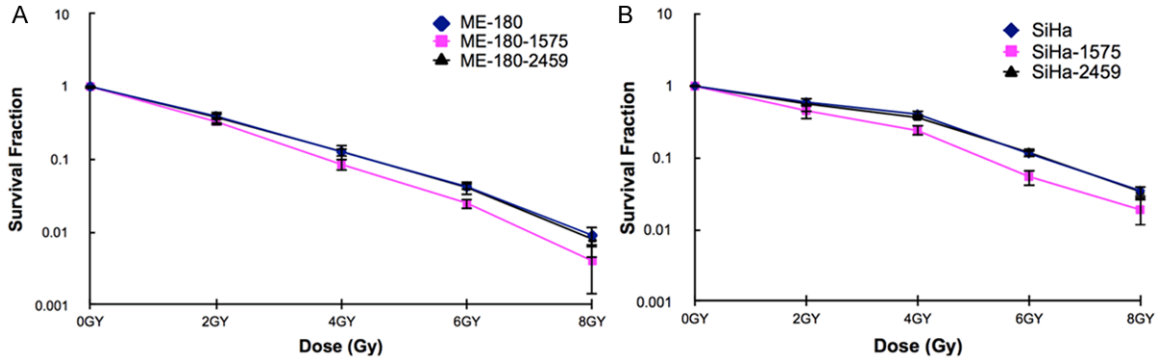

Figure 2. CD147 leads to radioresistance in cervical cancer cells in vitro. Clonogenic assay was conducted to examine the radiosensitivity of the cell lines. A. Survival curves of ME-180 cell lines after receiving 2 Gy, 4 Gy, 6 Gy and 8 Gy of radiation. The lowermost curve represents the survival curve of ME-180-1575 cells; the 2 overlapping curves at the top represent the survival curves of ME-180-2459 cells and ME-180 cells. B. Survival curves of SiHa cell lines after receiving 2 Gy, 4 Gy, 6 Gy and 8 Gy of radiation. The lowermost curve represents the survival curve of SiHa-1575 cells; the 2 overlapping curves at the top represent the survival curves of SiHa-2459 cells and SiHa cells. No significant differences in radiosensitivity were detected between cell lines that were stably transduced with CD147-cDNA (SiHa-2459 and ME-180-2459) and the untransduced parental SiHa and ME-180 cells.

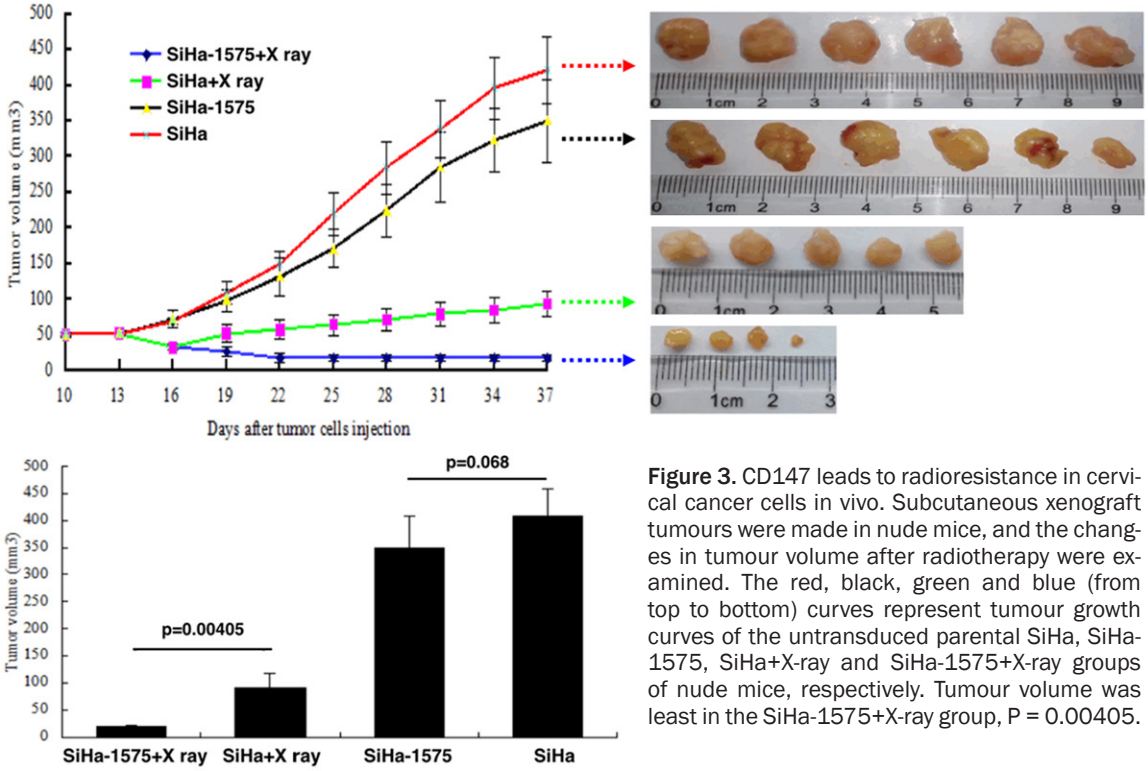

Figure 3. CD147 leads to radioresistance in cervical cancer cells in vivo. Subcutaneous xenograft tumours were made in nude mice, and the changes in tumour volume after radiotherapy were examined. The red, black, green and blue (from top to bottom) curves represent tumour growth curves of the untransduced parental SiHa, SiHa-1575, SiHa+X-ray and SiHa-1575+X-ray groups of nude mice, respectively. Tumour volume was least in the SiHa-1575+X-ray group, P = 0.00405.

were stably transduced with lentivirus-carrying cDNA-CD147 (-2459 cell lines) expressed CD-147 at levels similar to those of the parental cells. In contrast, short hairpin RNA (shRNA)-CD147 inhibited CD147 expression by more than 90% (cell lines -1575 or -1576). The results are shown in the **Figure 1**.

CD147 leads to radioresistance in cervical cancer cells in vitro

The effects of CD147 on the radiosensitivity of cervical cancer cells were examined in vitro using a clonogenic assay. The results are shown in the **Figure 2**. Silencing of CD147 gene expression in the cell lines of the experimental group (SiHa-1575 and ME-180-1575) resulted in increased radiosensitivity. Compared to the cell lines in the control group (SiHa, SiHa-2459, ME-180, and ME-180-2459), the survival curves of the experimental group were shifted to the left, no significant differences existed in the clonogenic capacities of the non-irradiated cell lines, the clonogenic capabilities of the cell lines were markedly reduced after irradiation, SF was significantly decreased in cells that received 4 Gy, 6 Gy and 8 Gy of radiation statistically ($P < 0.05$). No significant differences in radiosensitivity were detected between cell lines that were stably transduced with CD147-cDNA (SiHa-2459 and ME-180-2459) and the untransduced parental SiHa and ME-180 cells.

CD147 leads to radioresistance in cervical cancer cells in vivo

In vitro experiments showed that silencing of CD147 gene expression in SiHa and ME-180 cell lines (SiHa-1575 and ME-180-1575) resulted in increased radiosensitivity (**Figure 3**). This increase was more significant in the radioresistant SiHa cell lines. RNA and protein analyses showed that the CD147 gene was expressed at similar levels in cDNA-CD147-transduced cell lines and their parental cell lines. In addition, the radiosensitivity curves of the cell lines virtually overlapped. Therefore, the radioresistant cell lines SiHa and SiHa-1575 were used in the animal experiments to verify radiosensitivity and were used in the second half of the present study to investigate the mechanisms underlying radiosensitivity. SiHa and SiHa-1575 cells were inoculated subcutaneously into nude mice. The size of the xenograft tumours and changes in the size of the residual tumours after irradiation were recorded. The SiHa and SiHa-1575 groups contained 12 mice each. Tumour size and the time needed for tumouri-

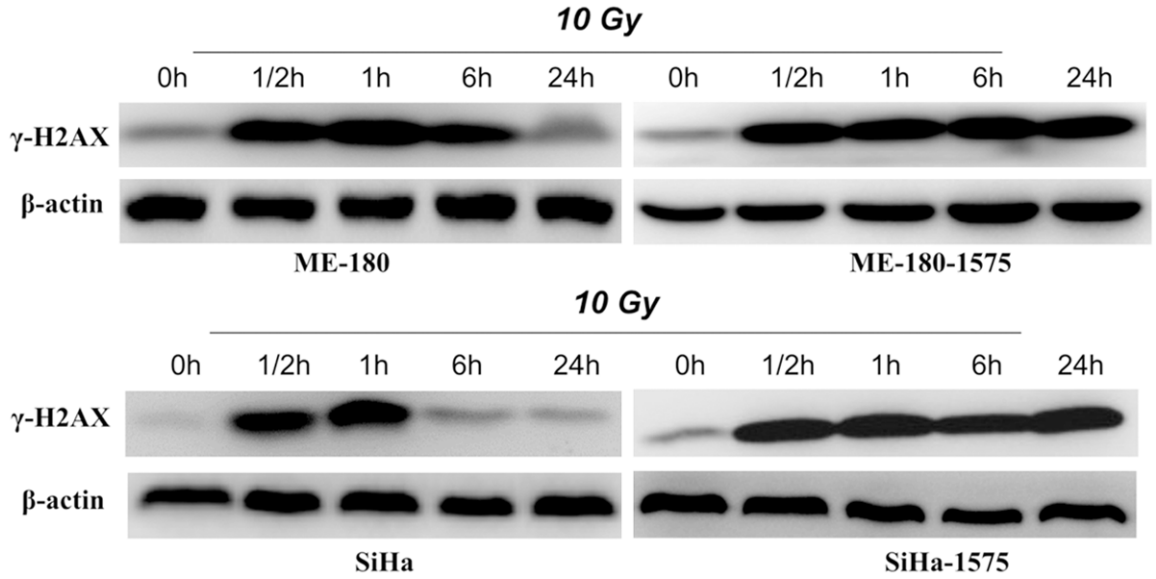

Figure 4. Silencing CD147 can affect DNA DSBs repair with elevating the expression of γH2AX. WEB examined the level of γH2AX in cell lines at different time after a single dose of 10 Gy irradiation. In ME-180 cell lines (upper panel), the level of γH2AX in untransduced parental ME-180 cells decreased at 6 h, and became barely detectable at 24 h. In contrast, the level of γH2AX in ME-180-1575 cells started to increase within 30 min after irradiation, reached a peak at 6 h, and remained at the peak level until at least 24 h after irradiation. In SiHa cells (lower panel), the level of γH2AX started to rise within 30 min after irradiation and decreased significantly after 1 h. In contrast, the level of γH2AX in SiHa-1575 cells rapidly increased within 30 min after radiation damage and remained at the peak level until at least 24 h after irradiation.

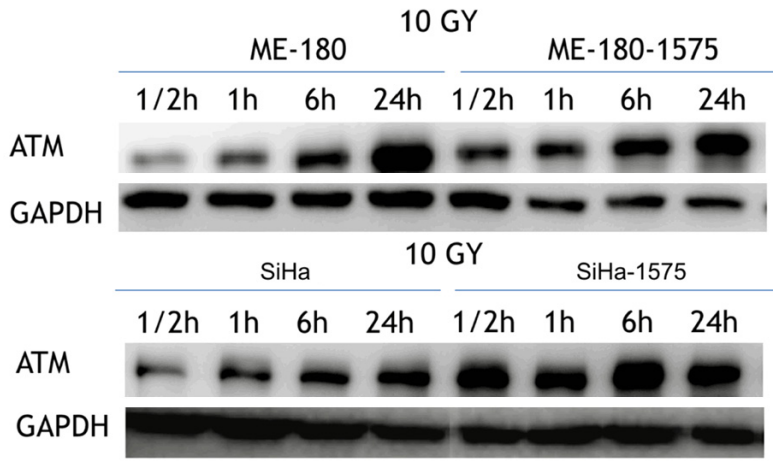

Figure 5. Silencing CD147 is not related to the expression of ATM in cell lines. WEB examined the level of ATM in cell lines at different time after a single dose of 10 Gy irradiation. At 30 min after radiotherapy, ATM expression levels were lower in ME-180 and SiHa cells than in ME-180-1575 and SiHa-1575 cells. However, ATM expression levels in cell lines were gradually elevated over time for ME-180, ME-180-1575 and SiHa cells. Eventually, there were no significant differences in ATM expression levels at 24 hours after irradiation.

genesis were recorded. On the 10th day of tumour growth (when the subcutaneous tumours had diameters of approximately 5 mm), the 12 tumour-bearing nude mice in Group A were randomly divided into two groups. One group received radiotherapy (16 Gy of 6-MV X-rays); the other did not. Mice in group B were subjected to the same treatments.

On the 16th day after inoculation of the tumour cells, no palpable tumours were found in one of the nude mice in the SiHa+X-ray group of nude mice, and this nude mice was ruled out of the group for statistic analysis. Two nude mice in the SiHa-1575+X-ray group died, one on the 18th day and the other on the 20th day, and these two nude mice were also ruled out. On the 37th day after inoculation of the tumour cells, all nude mice were killed. The mean tumour volumes in the SiHa, SiHa-1575, SiHa +X-ray and SiHa-1575+X-ray groups were 408 ±50.20, 350±57.34, 89.9±26.65 and 17.76± 4.15, respectively. Tumour volume was lower in

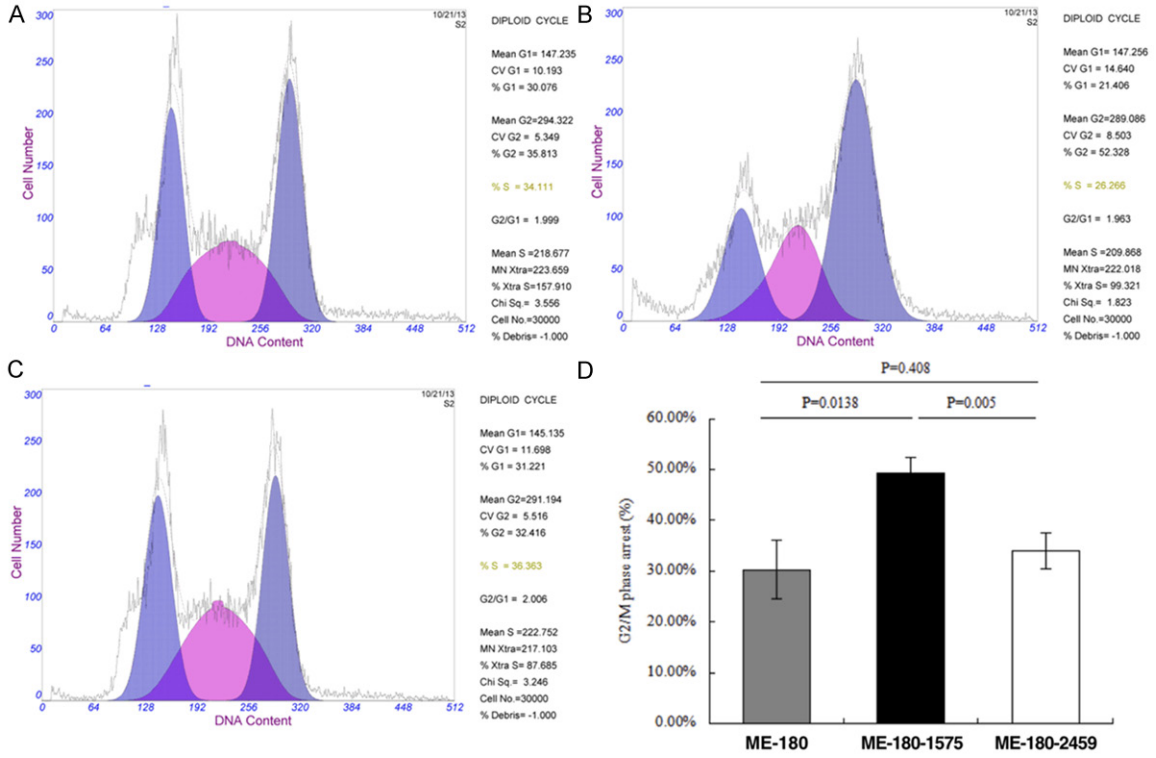

Figure 6. Silencing CD147 leads to G2/M phase arrest of the cell cycle after irradiation. Flow cytometry was employed to analyse the cell cycle of ME-180 cell lines after irradiation. A. ME-180 untransduced parental cell; B. shRNA-CD147-transduced CD147-negative cell line ME-180-1575; C. cDNA-CD147-transduced CD147-positive cell line ME-180-2459. ME-180-1575 contained a significantly higher percentage of cells in the G2/M phase of the cell cycle; D. The *P* values for these differences were 0.0138 and 0.005, respectively.

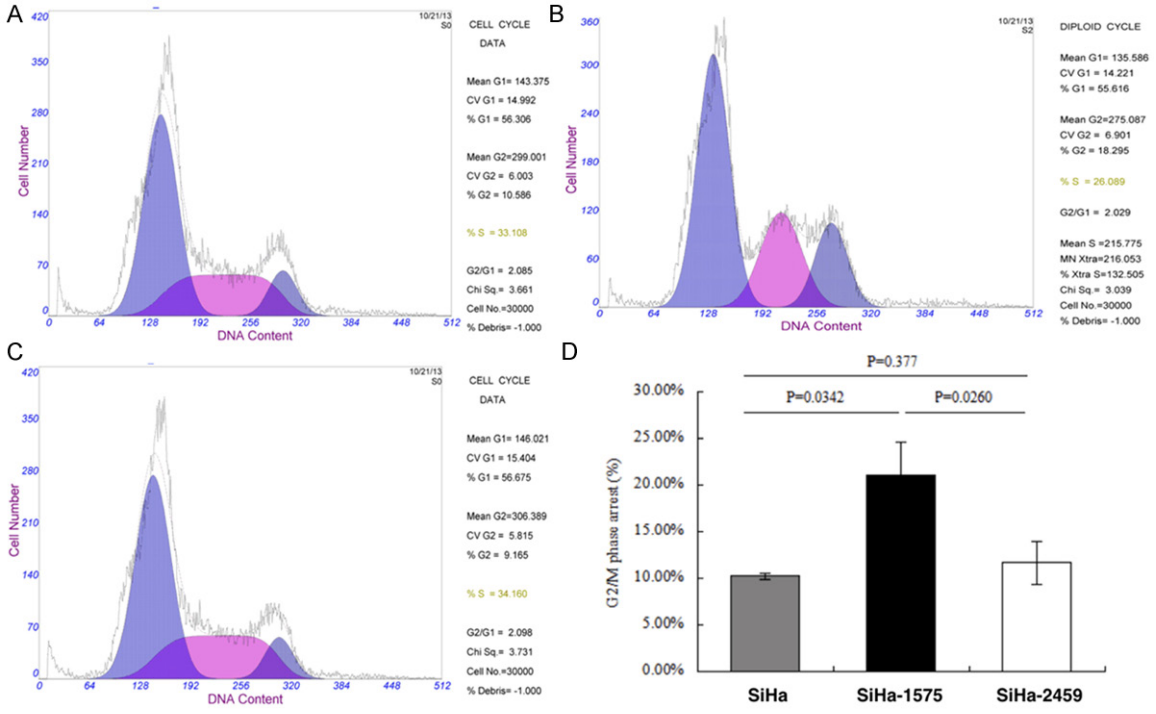

Figure 7. Silencing CD147 leads to G2/M phase arrest of the cell cycle after irradiation. Flow cytometry was employed to analyse the cell cycle of SiHa cell lines after irradiation. A. SiHa untransduced parental cell; B. shRNA-CD147-transduced CD147-negative cell line SiHa-1575; C. cDNA-CD147-transduced CD147-positive cell line SiHa-2459. The SiHa-1575 cells contained a significantly higher percentage of cells in the G2/M phase; D. The *P* values of these differences were 0.0342 and 0.0260, respectively.

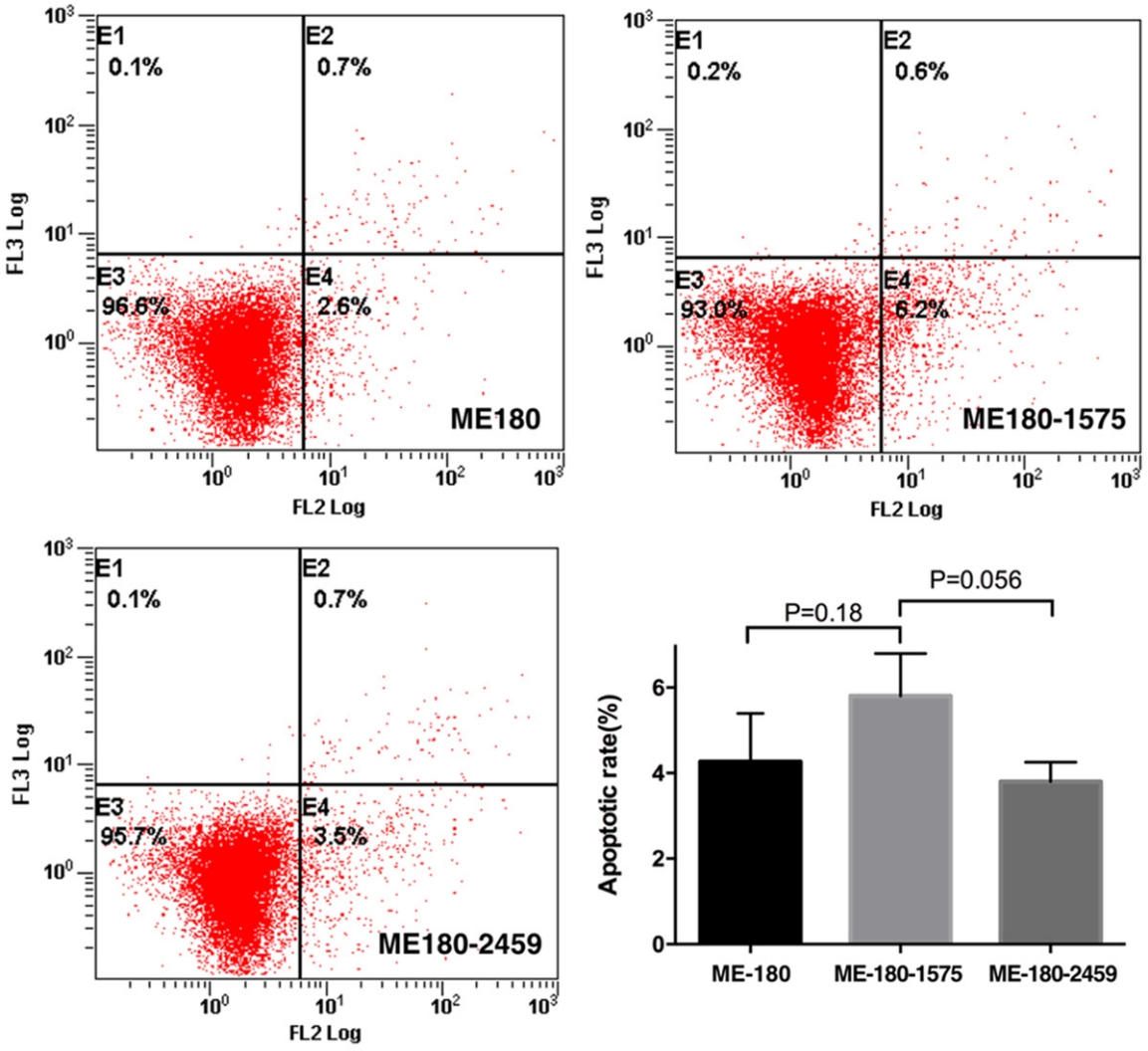

Figure 8. Silencing CD147 does not change the cell lines apoptosis after irradiation. Flow cytometry was employed to analyse ME-180 cell lines apoptosis after irradiation. The apoptotic rate in ME-180-1575 cells was compared to those in untransduced parental ME-180 and ME-180-2459 cells. The *P* values were 0.18 and 0.056, respectively.

the SiHa-1575 group than in the SiHa group. However, the difference was not statistically significant (P = 0.068). In contrast, tumour volume was significantly lower in the SiHa-1575+X-ray group than in the SiHa+X-ray group (P = 0.00405).

Silencing CD147 affects DNA DSBs repair

The expression of γH2AX and ATM in cancer cells post-radiotherapy can reflect the status of DNA DSBs repair. Therefore, cells were subjected to WB analysis to examine the expression levels of the γH2AX protein at 0 min, 30 min, 1 h, 6 h and 24 h after X-ray irradiation (6-MV X-ray beam). The results are shown in the **Figure 4**.

In ME-180 cells, the level of γH2AX started to rise within 30 min after a single dose of 10 Gy irradiation, decreased at 6 h, and became barely detectable at 24 h. In contrast, the level of γH2AX in ME-180-1575 cells started to

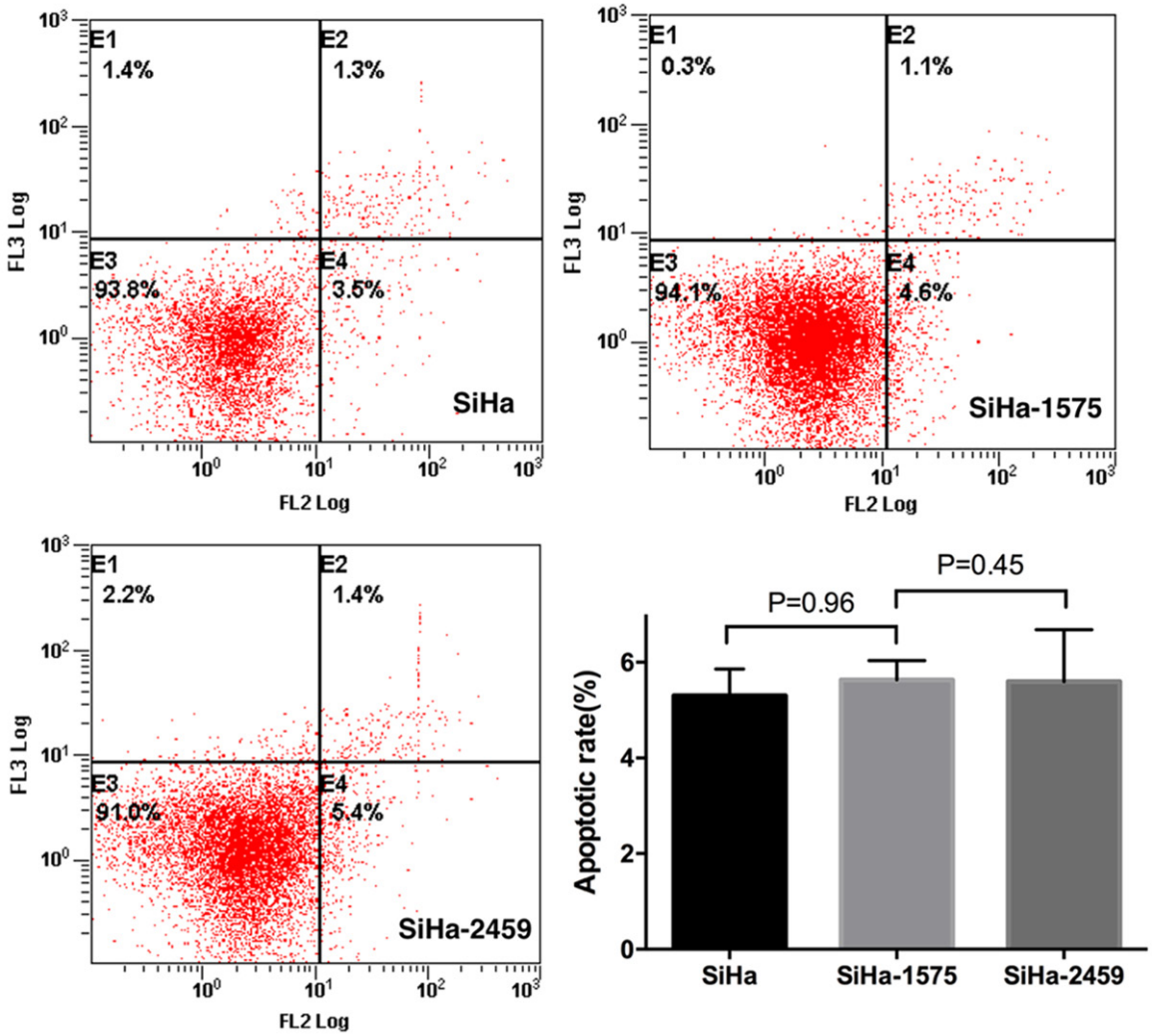

Figure 9. Silencing CD147 does not change the cell lines apoptosis after irradiation. Flow cytometry was employed to analyse SiHa cell lines apoptosis after irradiation. The apoptotic rate in SiHa-1575 cells was compared to those in untransduced parental SiHa and SiHa-2459 cells; the *P* values were 0.96 and 0.45, respectively, indicating that the differences were not statistically significant.

increase within 30 min after irradiation, reached a peak at 6 h, and remained at the peak level until at least 24 h after irradiation.

In SiHa cells, the level of γH2AX started to rise within 30 min after irradiation and decreased significantly after 1 h. In contrast, the level of γH2AX in SiHa-1575 cells rapidly increased within 30 min after radiation damage and remained at the peak level until at least 24 h after irradiation.

At 30 min after radiotherapy, ATM expression levels were lower in ME-180 and SiHa cells than in ME-180-1575 and SiHa-1575 cells. However, ATM expression levels in cell lines were gradually elevated over time for ME-180, ME-180-1575 and SiHa cells. Eventually, there were no significant differences in ATM expression levels at 24 hours after radiotherapy. The results are shown in the **Figure 5**.

Silencing CD147 changes the G2/M phase of the cell cycle after irradiation

Changes in cell cycle distribution after radiotherapy were analysed using flow cytometry. The percentage of cells in the G2/M phase was higher in the CD147-negative group than in the control group. The results are shown in the **Figures 6**, **7**.

After irradiation, the percentages of ME-180, ME-180-1575 and ME-180-2459 cells in the

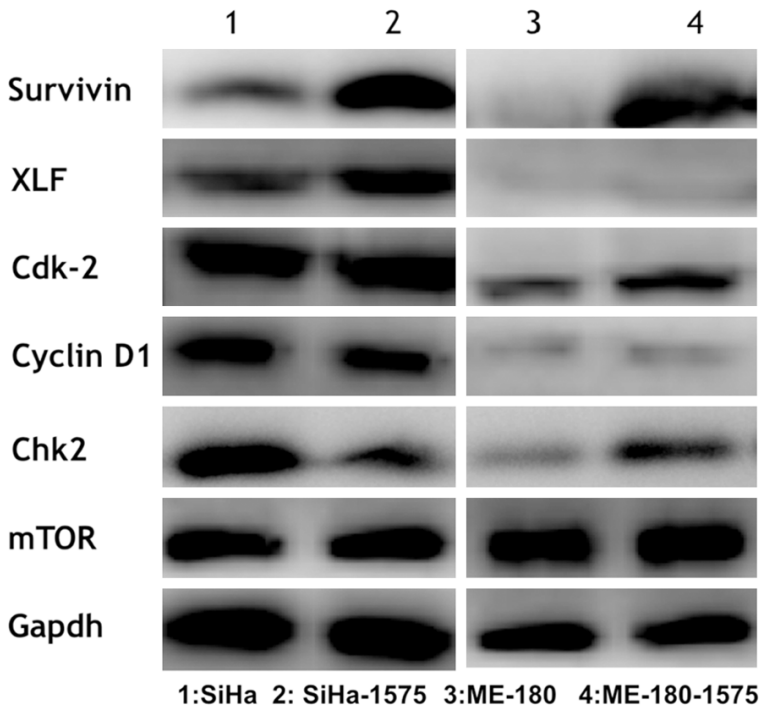

Figure 10. CD147 expression does not relate to some of the important proteins in apoptosis and cell cycle regulatory pathways. WB methods was used to examined the level of apoptosis inhibitory proteins and cell cycle regulatory proteins in cell lines, no certain relationship was found bwteen the expression of CD147 and these proteins. The apoptosis inhibitory proteins and cell cycle regulatory proteins were highly expressed in SiHa cells regardless of whether CD147 was expressed. ME180 cells: Xlf and cyclin D1 were not expressed. No significant difference was detected in cdk-2 or mTOR expression levels before and after blocking CD147 expression. Survivin was not expressed before the blockade of CD147 expression but was strongly expressed after the blockade of CD147 expression. Chk2 expression was slightly upregulated after the blockade of CD147 expression.

G2/M phase were 30.3%, 49.3% and 34%, respectively. Compared to ME-180 and ME-180-2459 cells, ME-180-1575 contained a significantly higher percentage of cells in the G2/M phase of the cell cycle; the *P* values for these differences were 0.0138 and 0.005, respectively.

After irradiation, the percentages of SiHa, SiHa-1575 and SiHa-2459 cells in the G2/M phase of the cell cycle were 10.17%, 21% and 12%, respectively. Compared to SiHa and SiHa-2459 cells, the SiHa-1575 cells contained a significantly higher percentage of cells in the G2/M phase; the *P* values of these differences were 0.0342 and 0.0260, respectively.

Silencing CD147 does not change the cell lines apoptosis after irradiation

The post-irradiation changes in the apoptosis of the various cell lines were examined using flow cytometry. The results are shown in the **Figures 8**, **9**.

Flow cytometric analysis showed that the mean apoptotic rates in logarithmically growing ME-180-1575 cells, parental ME-180 cells and ME-180-2459 cells were 5.8±1.0%, 4.27±1.12% and 3.8±0.45%, respectively. The apoptotic rate in ME-180-1575 cells was compared to those in ME-180 and ME-180-2459 cells. The *P* values were 0.18 and 0.056, respectively. The mean apoptotic rates in logarithmically growing SiHa-1575 cells, SiHa cells and SiHa-2459 cells were 5.63±0.40%, 5.30±0.56% and 5.60±1.08%, respectively. The apoptotic rate in SiHa-1575 cells was compared to those in SiHa and SiHa-2459 cells; the *P* values were 0.96 and 0.45, respectively, indicating that the differences were not statistically significant.

Correlation between CD147 expression and proteins of apoptosis and cell cycle

Prior to irradiation, WB analysis was performed to examine the expression levels of apoptosis inhibitory proteins (such as survivin, Xlf and mTOR/FRAP) and cell cycle regulatory proteins (such as Cdk-2, Cyclin D1 and Chk2) in various cell lines. There was no significant correlation between the expression of these proteins and CD147 expression status. However, different expression patterns were observed between ME-180 and SiHa cells. The results are shown in the **Figure 10**.

The apoptosis inhibitory proteins and cell cycle regulatory proteins were highly expressed in SiHa cells regardless of whether CD147 was expressed.

Xlf and cyclin D1 were not expressed in ME180 cells. No significant difference was detected in cdk-2 or mTOR expression levels before and after blocking CD147 expression. Survivin was not expressed before the blockade of CD147

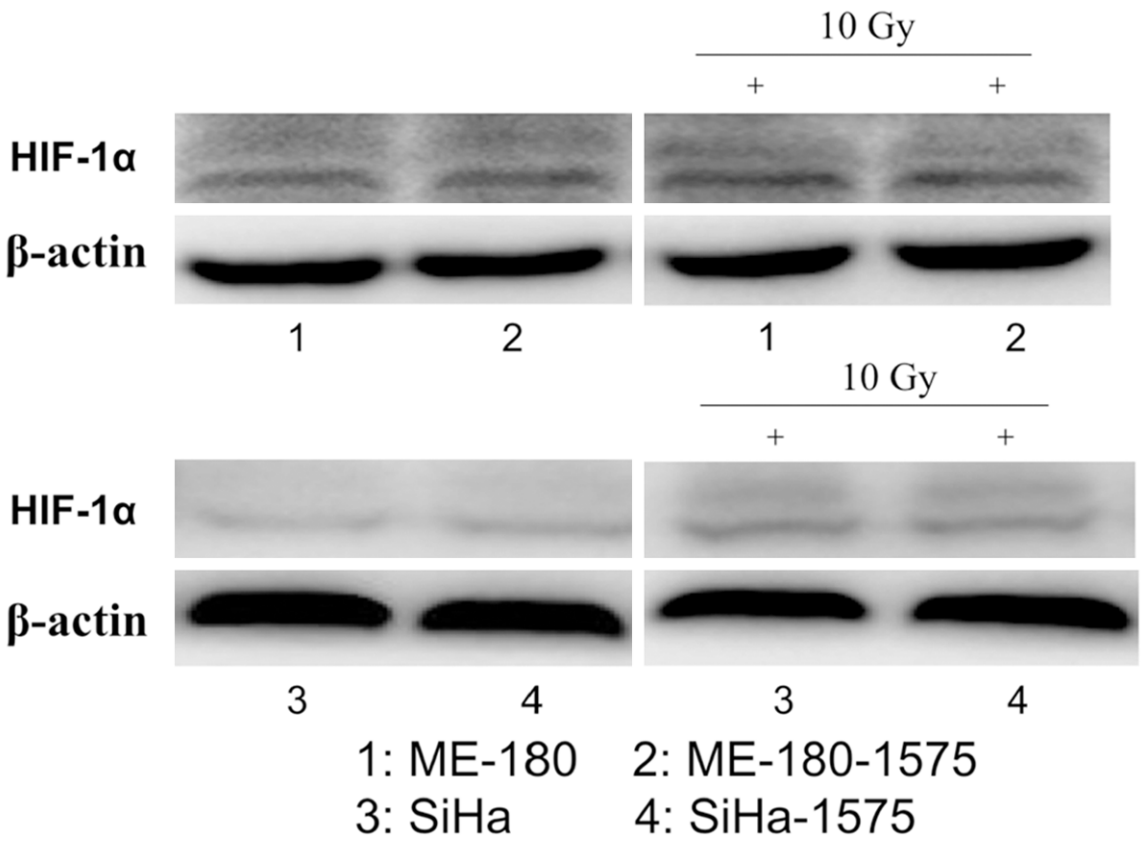

Figure 11. Silencing CD147 does not change the expression of HIF-1α in cell lines under hypoxic conditions. WEB examined the level of HIF-1α in cell lines at different time before and after a single dose of 10 Gy irradiation. WB analysis showed that the ME-180 and ME-180-1575 cells expressed low levels of HIF-1α, both before and after exposure to X-ray irradiation. Moreover, virtually no HIF-1α expression was detected in SiHa and SiHa-1575 cells.

expression but was strongly expressed after the blockade of CD147 expression. Chk2 expression was slightly upregulated after the blockade of CD147 expression.

Exression of CD147 and HIF-1α in cell lines under hypoxic conditions after silencing CD147

The experimental group (ME-180-1575 and SiHa-1575 cells) and the control group (ME-180 and SiHa cells) were cultured under hypoxic conditions (0.02% O_2) for 1 week. Each cell line was cultured in 2 dishes. One dish of each cell line was used for total protein extraction. The other dish was exposed to 10 Gy of X-ray irradiation (6-MV X-ray beam). At 24 h after irradiation, total cellular protein was isolated. WB analysis showed that the ME-180 and ME-180-1575 cells expressed low levels of HIF-1α, both before and after exposure to X-ray irradiation. Moreover, virtually no HIF-1α expression was detected in SiHa and SiHa-1575 cells. The results are shown in the **Figure 11**.

Discussion

In the present study, in vitro experiments showed that CD147 expression was correlated with radioresistance in cervical cancer cell lines, a finding that is consistent with the results of our previous clinical study. We demonstrated that CD147 expression is related to radiosensitivity in patients with cervical cancer, such patients generally showed poor prognosis, CD147 represents an adverse prognostic factor [8]. Huang et al. conducted a immunohistochemical study and found that CD147 expression is correlated with radiosensitivity and progression-free survival (PFS) in patients with cervical cancer [14], a finding that is also consistent with the results of our previous clinical study. A study conducted by Wu et al. shows that knocking out CD147 expression increases the radiosensitivity of SMMC-7721 and HepG2 hepatocellular carcinoma cells and suppresses the proliferative and metastatic capability of hepatocellular carcinoma after radiotherapy

[15]. The present study also found that inhibiting CD147 expression enhanced the radiosensitivity of cervical cancer cell lines. This enhancement was more significant in radioresistant SiHa cells. Therefore, CD147 may be the main intrinsic factor that induces radioresistance in cervical cancer cells.

In the present study, in vivo experiments showed that the inhibition of CD147 expression affected the growth rate of xenograft tumours in nude mice. However, the effect was not significant. In contrast, the inhibition of CD147 expression significantly increased the rate of xenograft tumour regression after radiotherapy. Moreover, the post-radiotherapy tumour regression rate was markedly reduced in nude mice with xenograft tumours expressing high levels of CD147. Using a nude mouse xenograft model of head and neck cancer, Dean et al. found that nude mice that had been treated with a CD147-specific antibody experienced delayed tumour growth in comparison with a control group [6]. Combined administration of the anti-CD147 antibody and radiotherapy in nude mice resulted in the most significant tumour regression. In addition, the growth of CD147-positive xenograft tumours in nude mice was not significantly inhibited after radiotherapy. The above findings are consistent with the results of the present study. To date, studies focusing on the mechanisms underlying CD147-mediated tumour radioresistance are very rare.

The present study found that after a single 10-Gy dose of irradiation, the levels of γH2AX rapidly decreased over time in cell lines that expressed high levels of CD147 (ME-180 and SiHa). In addition, the decrease occurred earlier in the SiHa cell line than in the ME-180 cell line. In ME-180 cells, the reduction in γH2AX levels occurred at 6 h after radiotherapy. In SiHa cells, the decrease in γH2AX levels occurred at 1 h after radiotherapy. This phenomenon may be related to the fact that ME-180 cells are inherently relatively radiosensitive, whereas SiHa cells are radioresistant. After the blockade of CD147 expression, the expression of γH2AX increased rapidly in both ME-180 and SiHa cells and reached maximal values at 30 min after radiation treatment. Afterward, the expression of γH2AX in both ME-180 and SiHa cells remained at the maximum level until 24 h after radiation treatment. The extent of post-radiotherapy cell death is directly related to radiotherapy-induced double-stranded DNA damage [16]. In irradiated cells, the time window for the repair of DNA damage is 4-6 h. During this period, cells suffering mild DNA damage complete damage repair and enter the proliferation cycle, whereas cells suffering severe or irreparable damage are induced to undergo apoptosis [17]. Intracellular γH2AX levels are a marker for DNA DSBs [9]. The present study found that γH2AX expression was higher in cervical cancer cells with blocked CD147 expression after radiotherapy than in the CD-147-positive group, indicating that CD147 may play an important role in the regulation of DNA DSBs repair after radiotherapy. CD147 may directly participate in DNA DSBs repair, thereby mediating radioresistance in cervical cancer cells.

The results also showed that ATM expression was increased in the CD147-negative group (ME-180-1575 and SiHa-1575 cells) shortly after radiotherapy. However, the expression of ATM in both cell types increased gradually over time. Eventually, there was no significant difference in ATM expression between these cell types. It is likely that ATM-mediated nonhomologous end-joining repair was partially upregulated. However, the role of ATM in the repair of radiation-induced damage is rather complex. In cells suffering radiation-induced injury, ATM participates in DNA damage checkpoint pathways, which not only initiate the apoptotic process to induce cell death but also protect cells from apoptosis [18]. ATM dysfunction leads to impaired DNA repair capacity. The regulation of ATM by CD147 and the specific role of ATM under CD147 regulation warrants further investigation.

The results also showed that the percentage of cells in the G2/M phase of the cell cycle was significantly increased in the CD147-negative group (ME-180-1575 and SiHa-1575 cells) in comparison to the CD147-positive group. Cells in different phases of the cell cycle display different sensitivity to radiotherapy. Cells arrested at the G1/S phase show a tendency towards being radioresistant, whereas cells arrested at the G2/M phase show a tendency to be radiosensitive [19]. CD147 may participate in the regulation of radioresistance through cell cycle arrest. Therefore, we preliminarily examined representative factors in cell cycle checkpoints.

The regulatory proteins involved in cell cycle checkpoints, cyclins/cyclin-dependent kinases (CDKs), are the main factors that regulate cell cycle progression and direct apoptosis. Among the cyclin/Cdk complexes, Cyclin E-Cdk-2 promotes entry into the S phase, whereas cyclin A-Cdk-2 exerts the opposite effect [20]. Cdk-2 expression induces a prolonged S phase in malignant tumours, allowing self-repair of the radiation-induced damage in tumour cells. Checkpoint kinases (Chks) promote single-strand DNA repair in various cell cycle phases, including the G1/S, S and G2/M phases, and even in the mitochondrial phase. Chks are core repair enzymes in DNA damage response pathways [21]. In the present study, we examined the levels of cell cycle proteins including Cdk-2, cyclin D1 and Chk2. Cyclin D1 and Cdk2 were strongly expressed in SiHa cell lines but were weakly or not expressed in ME-180 cells, regardless of whether CD147 expression was blocked. Chk2 expression was increased only in ME-180-1575 cells. Therefore, it is likely that CD147 does not regulate cell cycle progression through these key cell cycle regulatory proteins described above or that other regulatory proteins are also involved. The specific mechanisms involved also warrant further investigation.

In tumour cells, radiation-induced damage triggers apoptosis-related pathways. Cells that harbour repairable damage enter the repair process, whereas cells suffering irreparable damage enter the apoptotic program [17]. Reduced apoptosis and the downexpression of apoptosis-related proteins represent other important reasons underlying the radioresistance of malignant tumours. In the present study, the expression of the apoptosis-related protein ATM was slightly downregulated in CD147-negative cells, whereas the expression of the apoptosis inhibitory protein survivin was upregulated in CD147-negative cell lines. In addition, flow cytometric analysis showed no significant difference in apoptotic rate between the CD147-negative and CD147-positive groups. Therefore, it is likely that CD147 exerts no significant effect on the apoptosis of cervical cancer cells and does not affect the radiosensitivity of cancer cells through apoptotic pathways.

In the present study, we examined the differences in HIF-1α expression before and after the blockade of CD147 expression under hypoxic conditions. It was found that HIF-1α was not expressed by SiHa and ME-180 cell lines, regardless of the expression level of CD147. Therefore, it is likely that CD147-mediated radioresistance in cervical cancer cells is independent of the expression of hypoxia-inducible factors. Researchers have found that the promoter region of CD147 contains a special element known as the hypoxia-responsive element (HRE), which directly binds to HIF-1 [22]. In addition, CD147 acts in synergy with monocarboxylate transporter 1 (MCT1) or monocarboxylate transporter 4 (MCT4) to transport lactic acid, thus regulating the tumour microenvironment [23]. A recent study has found that cancer cells predominantly employ glycolysis for energy production even under aerobic conditions, a phenomenon known as the “Warburg effect” [13]. The mechanisms by which lactic acid and the pH of the tumour microenvironment affect the efficacy of radiochemotherapy are somewhat complex. It is likely that distinct mechanisms exist in different tumour cells [24]. Therefore, the role of CD147 under hypoxic conditions warrants further investigation.

The present study further demonstrated that CD147 is an intrinsic factor that is capable of inducing radioresistance in cervical cancer cells. The present study discovered for the first time that CD147 might mediate radioresistance in cervical cancer cells by regulating DNA DSBs repair and controlling cell cycle progression. In addition, the targeted inhibition of CD147 increased the radiosensitivity of cervical cancer xenografts. Therefore, CD147 may serve as a potential radiosensitizer in future. Although the present study comprehensively explored the potential mechanisms underlying the CD147-induced radioresistance in cervical cancer cells from the perspective of different pathways the study remains superficial. Future in-depth investigation into each of the pathways will be necessary to fully understand this topic.

Acknowledgements

The present study was supported by the National Natural Science Foundation of China (Youth Fund no. 81101954). The authors would like to thank Professor Jinming Yang (School of Medicine, University of Pennsylvania, USA) for his support and help during the design and completion of this work. The authors would also like to thank Jianmin Luo at the Central Laboratory of Fudan University, whose support

and help contributed to the successful completion of this work.

Address correspondence to: Xiaohua Wu, Department of Gynecologic Oncology, Fudan University Shanghai Cancer Center, 270 Dong-An Road, Shanghai 200032, China. Fax: +862164220677; E-mail: docwuxh@hotmail.com

References

[1] SEER Cancer Statistics Review 1975-2011. http://surveillance.cancer.gov/joinpoint/.

[2] Li J, Kang LN, Qiao YL. Review of the cervical cancer disease burden in mainland China. Asian Pac J Cancer Prev 2011; 12: 1149-53.

[3] Friedlander M, Grogan M; U.S. Preventative Services Task Force. Guidelines for the treatment of recurrent and metastatic cervical cancer. Oncologist 2002; 7: 342-7.

[4] Leitao MM Jr, Chi DS. Recurrent cervical cancer. Curr Treat Options Oncol 2002; 3: 105-11.

[5] Xiong L, Edwards CK 3rd, Zhou L. The biological function and clinical utilization of CD147 in human diseases: a review of the current scientific literature. Int J Mol Sci 2014; 15: 17411-41.

[6] Dean NR, Newman JR, Helman EE, Zhang W, Safavy S, Weeks DM, Cunningham M, Snyder LA, Tang Y, Yan L, McNally LR, Buchsbaum DJ, Rosenthal EL. Anti-EMMPRIN monoclonal antibody as a novel agent for therapy of head and neck cancer. Clin Cancer Res 2009; 15: 4058-65.

[7] Matsudaira H, Asakura T, Aoki K, Searashi Y, Matsuura T, Nakajima H, Tajiri H, Ohkawa K. Target chemotherapy of anti-CD147 antibody-labeled liposome encapsulated GSH-DXR conjugate on CD147 highly expressed carcinoma cells. Int J Oncol 2010; 36: 77-83.

[8] Ju XZ, Yang JM, Zhou XY, Li ZT, Wu XH. EMMPRIN expression as a prognostic factor in radiotherapy of cervical cancer. Clin Cancer Res 2008; 14: 494-501.

[9] Essers J, van Steeg H, de Wit J, Swagemakers SM, Vermeij M, Hoeijmakers JH, Kanaar R. Homologous and non-homologous recombination differentially affect DNA damage repair in mice. EMBO J 2000; 19: 1703-10.

[10] Reinhardt HC, Yaffe MB. Kinases that control the cell cycle in response to DNA damage: Chk1, Chk2, and MK2. Curr Opin Cell Biol 2009; 21: 245-55.

[11] Akli S, Bui T, Wingate H, Biernacka A, Moulder S, Tucker SL, Hunt KK, Keyomarsi K. Low-molecular-weight cyclin E can bypass letrozole-induced G1 arrest in human breast cancer cells and tumors. Clin Cancer Res 2010; 16: 1179-90.

[12] Carracedo A, Pandolfi PP. The PTEN-PI3K pathway: of feedbacks and cross-talks. Oncogene 2008; 27: 5527-41.

[13] Lu H, Forbes RA, Verma A. Hypoxia-inducible factor 1 activation by aerobic glycolysis implicates the Warburg effect in carcinogenesis. J Biol Chem 2002; 277: 23111-5.

[14] Huang XQ, Chen X, Xie XX, Zhou Q, Li K, Li S, Shen LF, Su J. Co-expression of CD147 and GLUT-1 indicates radiation resistance and poor prognosis in cervical squamous cell carcinoma. Int J Clin Exp Pathol 2014; 7: 1651-66.

[15] Wu J, Li Y, Dang YZ, Gao HX, Jiang JL, Chen ZN. HAb18G/CD147 promotes radioresistance in hepatocellular carcinoma cells: a potential role for integrin beta1 signaling. Mol Cancer Ther 2015; 14: 553-63.

[16] Lewanski CR, Gullick WJ. Radiotherapy and cellular signalling. Lancet Oncol 2001; 2: 366-70.

[17] Willers H, Dahm-Daphi J, Powell SN. Repair of radiation damage to DNA. Br J Cancer 2004; 90: 1297-301.

[18] Bucher N, Britten CD. G2 checkpoint abrogation and checkpoint kinase-1 targeting in the treatment of cancer. Br J Cancer 2008; 98: 523-8.

[19] Dillon MT, Good JS, Harrington KJ. Selective targeting of the G2/M cell cycle checkpoint to improve the therapeutic index of radiotherapy. Clin Oncol (R Coll Radiol) 2014; 26: 257-65.

[20] Woo RA, Poon RY. Cyclin-dependent kinases and S phase control in mammalian cells. Cell Cycle 2003; 2: 316-24.

[21] Smith J, Tho LM, Xu N, Gillespie DA. The ATM-Chk2 and ATR-Chk1 pathways in DNA damage signaling and cancer. Adv Cancer Res 2010; 108: 73-112.

[22] Ke X, Fei F, Chen Y, Xu L, Zhang Z, Huang Q, Zhang H, Yang H, Chen Z, Xing J. Hypoxia upregulates CD147 through a combined effect of HIF-1alpha and Sp1 to promote glycolysis and tumor progression in epithelial solid tumors. Carcinogenesis 2012; 33: 1598-607.

[23] Walters DK, Arendt BK, Jelinek DF. CD147 regulates the expression of MCT1 and lactate export in multiple myeloma cells. Cell Cycle 2013; 12: 3175-83.

[24] Grotius J, Dittfeld C, Huether M, Mueller-Klieser W, Baumann M, Kunz-Schughart LA. Impact of exogenous lactate on survival and radioresponse of carcinoma cells in vitro. Int J Radiat Biol 2009; 85: 989-1001.